• Basic Research •

Niosome-encapsulated auraptene reduced the mRNA expression of *VEGF-A* and *PDGFs* genes in human retina-derived RPE cell line

Akram Vahidi[1], *Teymoor Khosravi*[1], *Farzad Dastaviz*[1], *Mehdi Sheikh Arabi*[2], *Ayyoob Khosravi*[3,4], *Morteza Oladnabi*[3,5]

[1]Student Research Committee, Golestan University of Medical Sciences, Gorgan 4934174611, Iran
[2]Department of Medical Nanotechnology, Faculty of Advanced Medical Technologies, Golestan University of Medical Sciences, Gorgan 4934174611, Iran
[3]Stem Cell Research Center, Golestan University of Medical Sciences, Gorgan 4934174611, Iran
[4]Department of Molecular Medicine, Faculty of Advanced Medical Technologies, Golestan University of Medical Sciences, Gorgan 4934174611, Iran
[5]Gorgan Congenital Malformations Research Center, Golestan University of Medical Sciences, Gorgan 4934174611, Iran
Correspondence to: Morteza Oladnabi. Department of Medical Genetics, School of Advanced Technologies in Medicine, Golestan University of Medical Sciences, Gorgan 4934174611, Iran. Oladnabidozin@yahoo.com
Received: 2023-10-25 Accepted: 2024-03-04

Abstract

● **AIM:** To evaluate the effect of auraptene (AUR) treatment in forms of free and encapsulated in niosome nanoparticles by investigating the mRNA expression level of vascular endothelium growth factor (VEGF)-A and platelet-derived growth factors (PDGFs) in human retinal pigment epithelium (RPE) cell line.

● **METHODS:** Niosome nanocarriers were produced using two surfactants Span 60 and Tween 80. RPE cell line was treated with both free AUR and niosome-encapsulated. Optimum dosage of treatments was calculated using 3-(4,5-dimethylthiazol-2-yl)-2,5-diphenyltetrazolium bromide (MTT) assay. Expression of *VEGF-A* and *PDGF-A*, *PDGF-B*, *PDGF-C*, *PDGF-D* genes was measured after total RNA extraction and cDNA synthesis, using real-time polymerase chain reaction (RT-PCR).

● **RESULTS:** The highest entrapment efficiency (EE) was achieved by Span 60:cholesterol (1:1) with 64.3%. The half maximal inhibitory concentration (IC_{50}) of free and niosome-encapsulated AUR were 38.5 and 27.78 μg/mL, respectively. Release study revealed that niosomal AUR had more gradual delivery to the cells. RT-PCR results showed reduced expression levels of *VEGF-A*, *PDGF-A*, *PDGF-B*, *PDGF-C*, and *PDGF-D* after treatment with both free and niosomal AUR.

● **CONCLUSION:** Niosomal formulation of Span 60: cholesterol (1:1) is an effective drug delivery approach to transfer AUR to RPE cells. VEGF-A, PDGF-A, PDGF-B, PDGF-C, and PDGF-D are four angiogenic factors, inhibiting which by niosomal AUR may be effective in age-related macular degeneration.

● **KEYWORDS:** auraptene; niosome; age-related macular degeneration; angiogenesis; nanocarrier

DOI:10.18240/ijo.2024.06.06

Citation: Vahidi A, Khosravi T, Dastaviz F, Sheikh Arabi M, Khosravi A, Oladnabi M. Niosome-encapsulated auraptene reduced the mRNA expression of *VEGF-A* and *PDGFs* genes in human retina-derived RPE cell line. *Int J Ophthalmol* 2024;17(6):1028-1035

INTRODUCTION

Based on the 2019 global burden of disease study, age-related macular degeneration (AMD), along with cataracts, diabetic retinopathy, and glaucoma, are the four leading causes of vision impairment[1]. AMD is a progressive, irreversible, multifactorial condition that leads to central blindness and affecs around 170 million people worldwide[2]. Based on Centers for Disease Control and Prevention (CDC) data, 2 percent of individuals aged 40–44y and more than 46 percent of people over 85y are living with AMD, suggesting that the risk increases with age[3]. Drusen (a German word for “node”) is the yellowish accumulation of extracellular lipids and proteins between the retinal pigment epithelium (RPE) and the underlying Bruch’s membrane. Along with the gradual deterioration of photoreceptors, these two are the most common signs (not cause) of developing AMD[4]. Clinical classification of AMD is based on the size of drusen. Medium-sized (less than 124 μm) and large (more than 125 μm) drusen

are classified as early and intermediate AMD, respectively. The largest and pigmented drusen are seen at late AMD (also named advanced or neovascular). It is associated with fovea's geographical atrophy (GA) and significant loss of central vision[5]. The advanced AMD is divided into two groups: dry and wet. Dry AMD is defined by alterations in the Bruch membrane that promote atrophic cell death in photoreceptors, choriocapillaris, and RPE. If it leads to more rapid visual loss and development of macular neovascularization (a process with exudation and hemorrhage), the condition is called wet AMD. It has all the symptoms of dry AMD, plus the bleeding is not absorbed, and the invasion of fibrous-vascular tissue from the choroid and retinal blood vessels can soon result in loss of central vision[6]. Vascular endothelium growth factor (VEGF) is an essential mediator promoting angiogenesis in neovascularization in wet AMD[7]. Wet AMD is subdivided into choroidal neovascularization (CNV) and polypoidal choroidal vasculopathy (PCV). The former is an acute and destructive form of AMD marked by angiogenesis beneath the retina. Under normal conditions, endothelial cells in the blood vessels behind the retina do not proliferate and build new vessels under normal conditions. But during CNV, new blood capillaries grow abnormally in the choroid's capillary lamina, cross through the Bruch membrane, and penetrate the macula. They are highly permeable and fragile, so that leaked blood components accumulate under the macula. Therefore, it may shift from its original place, resulting in the formation of subretinal disciform scars. Inhibition of molecular mediators, including *VEGF-A* (Located on 6p21.1 with 26 transcipts) and platelet-derived growth factor (*PDGF*) genes (including *PDGF-A* on 7p22.3, *PDGF-B* on 22q13.1, *PDGF-C* on 4q32.1, and *PDGF-D* on 11q22.3), is a potential therapeutic strategy for wet AMD patients[8-9]. Nano-based drug delivery, photodynamic therapy, exosomes, gene and stem cell therapies are other options[10], as illustrated in Figure 1, studies have used different approaches against AMD, among which anti-VEGF and anti-PDGF methods have shown to be quite promising[11-15]. Auraptene (AUR), the best-known member of umbelliferone coumarins, is biosynthesized by fruits like lemon and grapefruit. It has well-established pharmacological and therapeutic effects in human diseases[16-19]. By reducing the mRNA expression of matrix metallopeptidase 2 (*MMP2*) and *MMP9* genes, AUR has been found to prevent the migration and invasion of cervical and ovarian cancer cells, as well as ulcerative colitis. In addition, Toliver *et al*[20] showed that AUR could prevent angiogenesis by blocking VEGF expression in human umbilical vein endothelial cells line. In another study by *Jang et al*[21] VEGF-induced neovascularization in nude mice reduced after AUR treatment *in vivo*. In the present study, we combined two AMD therapeutic strategies, nano-based drug delivery, and VEGF inhibitors. We aimed to establish a proper niosomal formulation to encapsulate AUR and deliver it to RPE cell line. Then, we evaluated the toxicity and mRNA profile of cells after treatment with free and niosomal AUR.

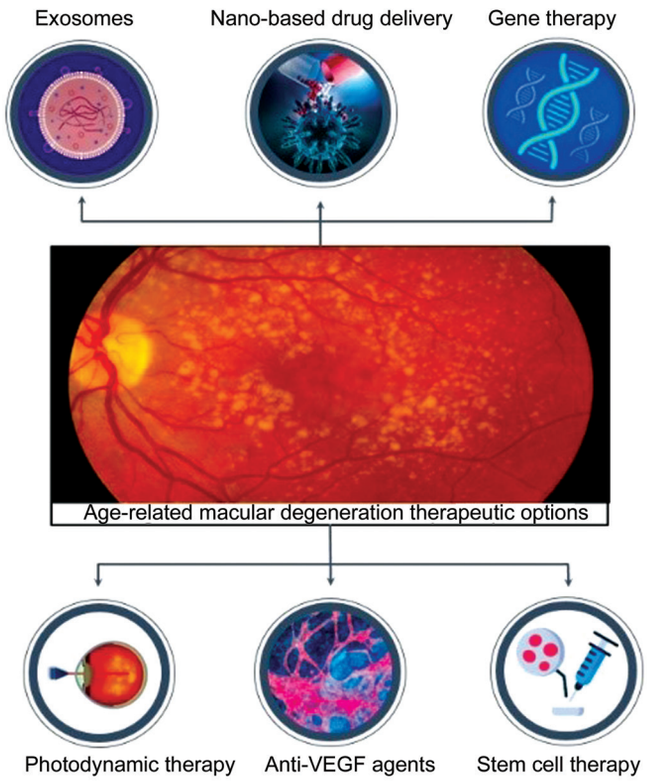

Figure 1 Age-related macular degeneration therapeutic strategies
VEGF: Vascular endothelium growth factor.

MATERIALS AND METHODS

Ethical Aproval The study was approved by the Ethics Committee of Golestan University of Medical Sciences (ethics code: IR.GOUMS.REC.1399.065).

Cell Culture The present study utilized an RPE cell line that had undergone prior isolation and culturing procedures in our previous investigation[22]. The cells were cultured in T-25 flasks containing a complete culture medium containing 10% fetal bovine serum (FBS) and incubated at 37°C and 5% CO_2 after thawing. Flasks with 90% confluency were utilized for cell passage or storage in a liquid nitrogen tank (-192°C). Treatments were carried out in flasks with 90% confluent cells. Briefly, cells were harvested using trypsin-ethylenediaminetetraacetic acid (EDTA) and seeded into well-plates.

Niosome Preparation Thin-film hydration was used to synthesize the niosomes using two non-ionic surfactants (Tween 80 and Span 60) and cholesterol. These components were dissolved in a round bottom balloon in 10 mL of an organic solution containing ethanol and chloroform in a 1:1 ratio. To generate a thin coating and evaporate organic solvents, a rotary vacuum pump device was used. The balloon contents were exposed to 50°C–60°C for 60min after

being hydrated with phosphate-buffered saline (PBS) buffer (pH=7.4). The solution was maintained at 25°C overnight to boost the chemical composition of AUR's absorption into the lipid membrane of niosomes. The niosome solution was filtered through a 0.22 nm syringe filter the next day, then sonicated for 10min before being stored in the refrigerator.

Auraptene Characteristics: EE, Size, Zeta Potential and Polydispersity Index To calculate the reference wavelength of AUR, ultraviolet (UV)-visible spectroscopy was used to examine different concentrations of the AUR. Then, a standard concentration was curved. At a wavelength of 323 nm, the light absorption of serially prepared quantities of AUR was measured. As a result, a standard curve representing the concentration of AUR was created. Maximum light absorption was achieved at a concentration of 100 µg/mL. To calculate entrapment efficiency (EE) of niosomal AUR, 5 mL of the niosome nanoparticle suspension was centrifuged at 13 000 rpm for 30min. Then, 2 mL of PBS buffer (pH=7.4) was used to wash the supernatant. The concentration of chemical compound in the solution was determined by measuring its absorption at 320 nm. The following formula was used to calculate the amount of encapsulated AUR:

$$\text{Niosomal auraptene EE}(\%)=\frac{\text{Amounts of Auraptene in the supernatant}}{\text{Total amounts of Auraptene}}\times 100$$

Furthermore, the dynamic light scattering (DLS) method was used to determine vesicle size, zeta potential, and polydispersity index (PDI) of niosome-encapsulated AUR.

***In Vitro* Release Study** The membrane diffusion method was used to determine the rate of AUR release from niosome nanoparticles. The 2 mL of the solution (10 kDa cut-off) was placed into a dialysis bag with 50 mL of PBS buffer (pH=7.4). It was shacked at 37°C and 40 rpm. At 0, 1, 2, 3, 4, 5, 6, 7, 8, 12, and 24h intervals, 2 mL of the solution around the dialysis sack was withdrawn and replaced with a new 2 mL PBS buffer. The absorbance of the collected solutions was measured at 320 nm. A standard curve was used to calculate the amount of AUR released at each moment, plotted against time.

Infrared Spectroscopy Centrifugation was used to extract AUR niosomal carriers from the suspension, and the surplus solution was evaporated. The samples were compacted into plates after being combined with potassium bromide (KBr). In order to explore the niosome functional groups, the fourier-transform infrared spectroscopy (FT-IR) spectra were scanned for samples in the wavelength range of 400–4000 cm^{-1}. The FT-IR spectra of the niosome system containing AUR were compared to that of the niosome system without AUR and free AUR to evaluate possible chemical interactions between niosome and AUR.

Transmission Electron Microscopy The surface morphology of the generated niosomal AUR was characterized using transmission electron microscopy (TEM H-9500). A solution of niosome-encapsulated AUR at concentration of 10 µg/mL was used.

IC_{50} Calculation The half maximal inhibitory concentration (IC_{50}) of a substance is defined as a concentration in which it blocks 50 percent of a biological function[23]. We used the 3-(4,5-dimethylthiazol-2-yl)-2,5-diphenyltetrazolium bromide (MTT) assay to assess cell viability. For that purpose, 3.5×10^4 RPE cells were seeded into 96-well plates, before treating with varying dosages of free and niosomal AUR (three repeats for each dosage), and 24h of incubation. An MTT assay was performed to analyze cell viability 24, 48, and 72h after treatment. The formed purple formazan crystals were dissolved in dimethyl sulfoxide (DMSO). An enzyme linked immunosorbent assay (ELISA) reader was used to assess light absorption at 570 nm. The cell viability was calculated according to the following formula:

$$\text{Cell viability}(\%)=\frac{\text{Absorption in the experimental wells–Background}}{\text{Absorption in the control wells}}\times 100$$

RNA Extraction, cDNA Synthesis, and RT-PCR RNA was extracted from $2–4\times10^5$ RPE cells treated with free niosome, free AUR, and niosomal AUR, according to the kit instructions (denazist, Iran). The purity of extracted RNA was measured using a nanodrop spectrophotometer. Pure extracted RNA was defined as a ratio of 260/280 and 260/230 optical densities (OD) between 1.8 and 2. We then used isolated total RNA to perform cDNA synthesis (Parstoos Inc. Kit). We implemented glyceraldehyde 3-phosphate dehydrogenase (GAPDH) housekeeping gene to normalize the expression levels. Also, agarose gel electrophoresis verified the accuracy of cDNA amplifications. The expression of *VEGF-A*, *PDGF-A*, *PDGF-B*, *PDGF-C*, *PDGF-D*, and *GAPDH* genes in cells treated with free niosome, free AUR, and niosomal AUR were measured using SYBR Green real-time polymerase chain reaction (RT-PCR, Yekta Tajhiz Azma Inc., Tehran, Iran). Table 1 contains the list of PCR primers[22,24-27].

Statistical Analysis The $2^{-\Delta\Delta Ct}$ method was used to calculate the relative fold changes in gene expressions. *GAPDH* gene was used as reference. The graphs were produced using the graphpad Prism software v9.0.0. Statistical differences in gene expression were evaluated using Student's *t*-test. Significant was defined as a *P*-value <0.05 with a 95% confidence interval (CI).

RESULTS

Niosomal Formulation with Cholesterol:Span 60 (1:1) Reached Highest EE Type of surfactant and the ratio of surfactant to cholesterol were examined to reach the optimum EE rate. Furthermore. We observed that the non-ionic surfactant Span 60 had higher EE than Tween 80. Also, at cholesterol:Span 60 ratios of 0:1, 0.5:1, 1:1, and 2:1, EE were 18.2%, 25%, 64.3%, and 41%, respectively. We continued the

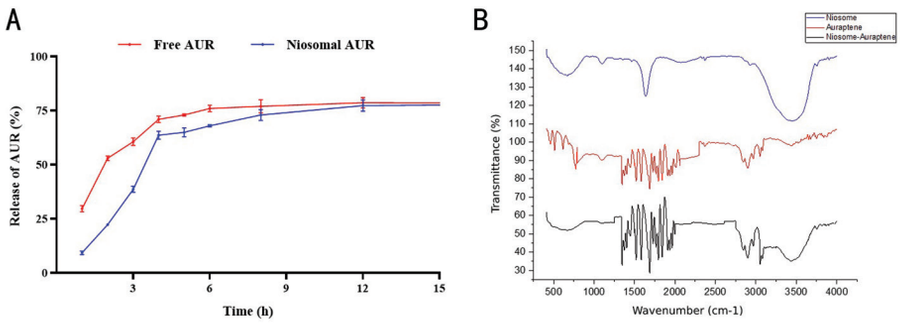

Figure 2 Characterization of auraptene-loaded niosomes A: *In vitro* release of free and niosomal AUR. All values are illustrated as mean (*n*=3). B: FT-IR spectrums of AUR-free niosome in blue, free AUR in red, and niosomal in black. AUR: Auraptene; FT-IR: Fourier-transform infrared spectroscopy.

Table 1 List of PCR oligonucleotide primers

Primers	Directions	Sequence (5′ to 3′)	Size of PCR product	Reference
GAPDH	Forward	5'-ACAGTCAGCCGCATCTTC-3'	317 bp	22
	Reverse	5'-CTCCGACCTTCACCTTCC-3'		
VEGF-A	Forward	5'-GGAGGGCAGAATCATCACGAA-3'	3151 bp	22
	Reverse	5'-GGTCTCGATTGGATGGCAGT-3'		
PDGF-A	Forward	5'-TCGATGAGATGGAGGGTCG-3'	71 bp	24
	Reverse	5'-ACCCGGACAGAAATCCAGTCT-3'		
PDGF-B	Forward	5'-CTCGATCCGCTCCTTTGATGA-3'	239 bp	25
	Reverse	5'-CGTTGGTGCGGTCTATGAG-3'		
PDGF-C	Forward	5'-GACTCAGGCGGAATCCAACC-3'	129 bp	26
	Reverse	5'-CTTGGGCTGTGAATACTTCCATT-3'		
PDGF-D	Forward	5'-CCCAGGAATTACTCGGTCAA-3'	105 bp	27
	Reverse	5'-ACAGCCACAATTTCCTCCAC-3'		

GAPDH: Glyceraldehyde-3-phosphate dehydrogenase; VEGF-A: Vascular endothelial growth factor A; PDGF-A: Platelet-derived growth factor A; PDGF-B: Platelet-derived growth factor B; PDGF-C: Platelet-derived growth factor C; PDGF-D: Platelet-derived growth factor D.

study using Cholesterol:Span 60 (1:1) formulation. Size, zeta potential, and scattering index of niosome formulations were measured using DLS.

Results of Release Study Figure 2A represents the amount of AUR released in free form and in niosomal formulation of cholesterol:Span 60 (1:1) in PBS buffer (pH=7.4) at different points in time. It demonstrates that the release rate was slower and more gradual in niosomal form compared to free form. The results also showed that after 4h 63.667%±3.21% of the drug was release from the niosomes.

FT-IR Results In the Span 60 structure of AUR-free niosomes, a peak of 3500 cm^{-1} belongs to a hydroxyl group (-OH), a peak of 1550 cm^{-1} belongs to carbonyl group (C=O), and a peak of 1020 cm^{-1} belongs to CO ester (C=O groups) were observed (blue line, Figure 2A). In addition, the structure of AUR (red line, Figure 2B) showed peaks of 3000 cm^{-1} and 2800 cm^{-1} corresponding to CH_2 alkanes, peaks of 1700 cm^{-1} belonging to C=C and C=O groups, and a peak of 1400 cm^{-1} corresponding to the esterified CO within the ring. Black line in Figure 2A shows the encapsulation of AUR by a Span 60-structured niosome. As a result, peaks related to Span 60 at 3500 cm^{-1} and 1550 cm^{-1} and peaks related to AUR at 3000 cm^{-1} and 1700 cm^{-1} are recognizable, indicating that AUR encapsulates

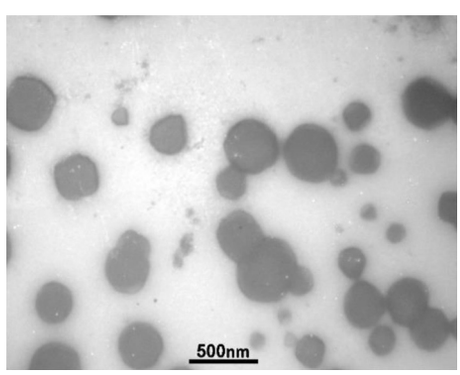

Figure 3 Image recorded using TEM of niosomal AUR TEM: Transmission electron microscopy; AUR: Auraptene.

in the niosome nanocarriers. Furthermore, the absence of a new peak and the disappearance of other previuos structural peaks indicate that the structure of AUR remains unchanged, that no chemical reaction occurs during the encapsulation process, and that AUR has retained its structure in the niosomal form.

TEM Image The surface morphology of AUR-containing niosomes was investigated using TEM microscopy. The spherical shapes of two lipid layers created by the aggregation of hydrophobic components are depicted in Figure 3.

IC_{50} Values To calculate the optimum dosage, MTT assay was performed on cells treated with free and niosomal AUR at

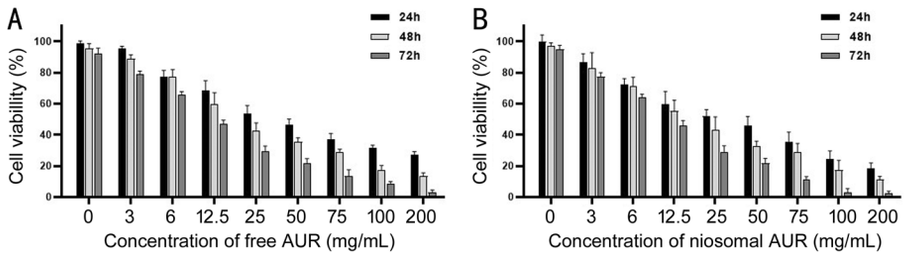

Figure 4 RPE cell line viability after treatment with free (A) and niosoma (B) AUR, at after 24, 48 and 72h time points AUR: Auraptene.

eight different concentrations (3, 6, 12.5, 25, 50, 75, 100, and 200 μg/mL), at 3 separate post-treatment intervals (24, 48, 72h). For free AUR the IC_{50} values at 24, 48, and 72h post-treatment were 38.5, 21.56, and 11.05 μg/mL, respectively. Moreover, for niosomal AUR, the IC_{50} values at 24, 48, and 72h post-treatment were 27.78, 18.56 and 10.6 μg/mL, respectively. The results demonstrated that both treatments had a dose-dependent but not time-dependent effects on the RPE cell line (Figure 4).

RT-PCR Results Based on MTT results, we used 38.5 μg/mL of free AUR and 27.78 μg/mL of niosomal AUR for a 24h treatment on RPE cell line. Expression level of *VEGF-A*, *PDGF-A*, *PDGF-B*, *PDGF-C*, and *PDGF-D* were quantified using RT-PCR. The results showed that niosomal AUR compared to free AUR, significantly reduced the mRNA expression level of the five genes (Figure 5).

DISCUSSION

In recent years nanocarriers like liposomes and niosomes have attracted attention in the field of drug delivery[28-29]. Niosomes are non-ionic lipid bilayer surfactant-based vesicles that have enhanced stability and biodegradability. Because of their small size, they can pass cellular barriers and successfully aggregate in the target region. Membrane permeability, increasing drug bioavailability, and high rate of EE have made them promising tools in pharmaceutical delivery systems[30-31]. Inhibiting angiogenesis can be an effective option to treat neovascular AMD[32]. Many efforts have been made in recent years. None has been more noticeable than anti-VEGF drugs. VEGF and PDGF superfamilies have been recent favorable targets in AMD therapy[33-35]. Various chemical compounds and drugs with anti-angiogenic effects have been explored to treat neovascular AMD, including pegaptanib, bevacizumab, and ranibizumab[36]. Recent studies showed that AUR efficiently inhibits endothelial cell migration, invasion, proliferation, and vascular development[37]. Also, AUR anti-angiogenesis activity has already been demonstrated[38-39]. Figure 6 graphically summarizes the procedure of this study.

Here, we prepared a cholesterol:Span 60 formulation of niosome and encapsulated AUR in the niosomes. Then, RPE cells were exposed to free and niosomal AUR. Our work aimed to investigate their anti-AMD potential by measuring the *VEGF-A* and *PDGFs* genes' expression levels. The addition of non-ionic surfactants in niosome formulations creates a substrate for trapping the chemical compound and gradually releasing it, which therefore lowers the dose of the desired chemical. Niosome formulation with Span 60 exhibited higher EE than formulation with Tween-80, which might be attributed to the hydrophilic-to-hydrophobic ratio[40]. The Span 60 formulation with the highest EE (64.3%) and surfactant to cholesterol ratio of 1:1 was used in this study. The hydrophobic AUR is trapped efficiently by the low hydrophobicity ratio of Span 60. Also, the 1:1 ratio prevents the formation of thin film and maintain EE, which seems to be a result of a competition between cholesterol and the hydrophobic AUR for placement within the bilayer membrane. These results were consistent with a previous study that showed nano-encapsulation of AUR with particles of solid lipid nanoparticles improves skin absorption and anti-inflammatory characteristics[41]. The results demonstrated that *VEGF-A*, *PDGF-A*, *PDGF-B*, *PDGF-C*, and *PDGF-D* expression levels in RPE cells were considerably lowered in cells treated with either niosome-encapsulated or free AUR. According to Mouse Genome Informatics (MGI) database, knocking down *VEGF-A* gene in mouse models can impair angiogenesis and blood-island formation. *PDGF-A* knockdown can result in incomplete cephalic closure and increased apoptosis of neural crest cells. *PDGF-B* knockdown can lead to the absence of microvascular pericytes and capillary aneurisms. Moreover, *PDGF-D* plays a critical role in the expression of vascular-differentiation related genes in embryonic stem cells. Our findings also reveal that niosomal AUR had more significant effect on the expression level of our genes of interest compared to free AUR. However, the mechanism(s) by which AUR may suppresses these genes remain unknown. In this regard, previous studies argued that this molecule is able to inhibit metalloproteinases, G1/S cell cycle checkpoint, and induce apoptosis[42]. Encapsulating AUR in niosome nanocarriers may be particularly efficient in preventing angiogenesis by lowering the expression of *VEGF-A* and *PDGF* genes in AMD[43].

There were some limitations in this work that should be reflected by future studies. First, there are other formulations of niosome that might have more efficiency than cholesterol:Span

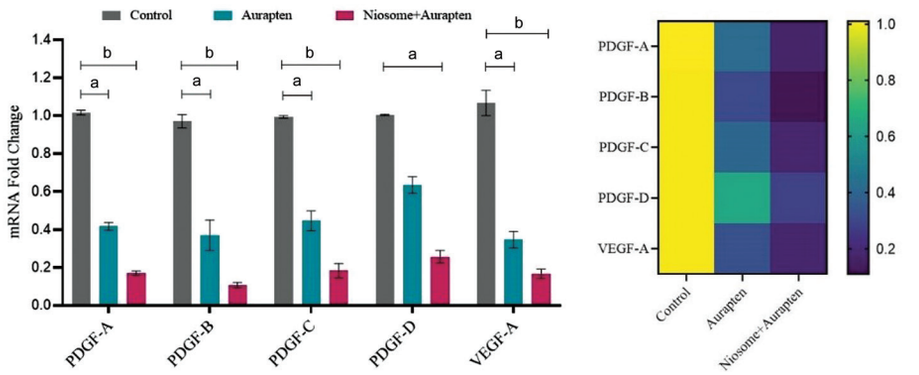

Figure 5 The mRNA expression levels of *VEGF-A*, *PDGF-A*, *PDGF-B*, *PDGF-C*, and *PDGF-D* in RPE cells treated with free and niosomal AUR, after 24h *P*<0.05 was assumed as significant quantity. VEGF: Vascular endothelium growth factor; PDGF: Platelet-derived growth factor; RPE: Retinal pigment epithelium; AUR: Auraptene. [a]*P*<0.05; [b]*P*<0.01.

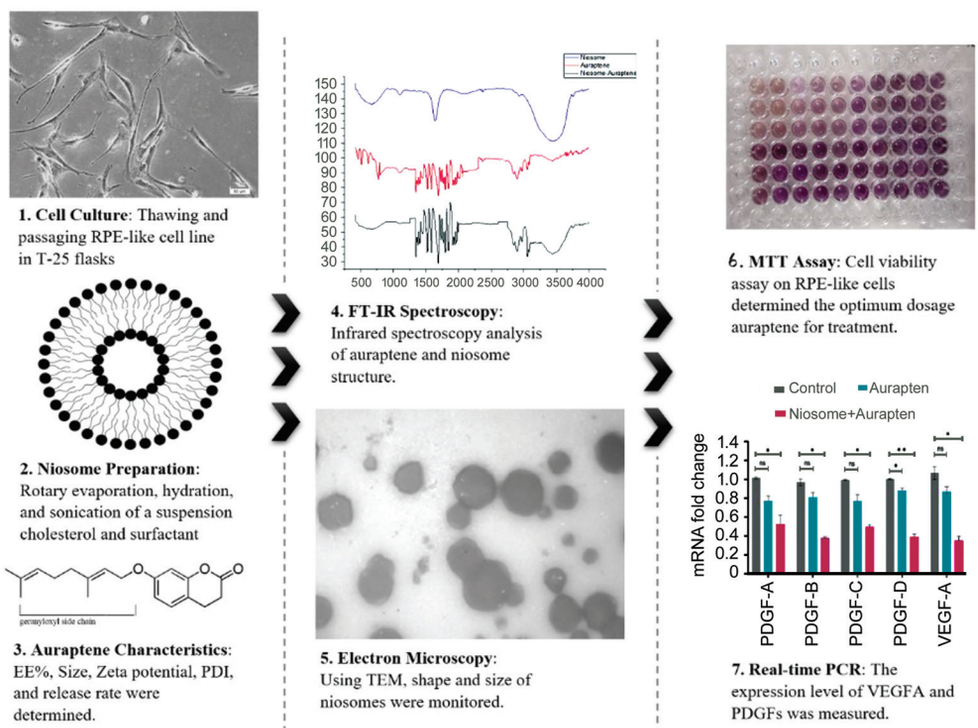

Figure 6 Study workflow and procedure RPE: Retinal pigment epithelium; VEGF: Vascular endothelium growth factor; PDGF: Platelet-derived growth factor; PCR: Polymerase chain reaction; EE: Entrapment efficiency; PDI: Polydispersity index; TEM: Transmission electron microscopy; FT-IR: Fourier-transform infrared spectroscopy; MTT: 3-(4,5-dimethylthiazol-2-yl)-2,5-diphenyltetrazolium bromide.

60. For instance, derivatives of niosome with pH sensitivity, and polymer modification worth to be included[44-45]. Moreover, the anti-AMD potential of AUR should be investigated in VEGF-A and PDGFs protein levels. Also, our investigation did not encompass the quantification of protein levels and the utilization of *in vivo* experimental models. Future research endeavors should contemplate these insightful recommendations, integrating both protein level assays and *in vivo* methodologies to yield a more holistic elucidation of the pharmacological implications of AUR.

ACKNOWLEDGEMENTS

Authors' contributions: Vahidi A: methodology, investigation, formal analysis, writing—original draft. Khosravi T: methodology, visualization, writing—original draft. Dastaviz F: methodology, investigation. Sheikh Arabi M: methodology, data curation. Khosravi A: methodology, data curation. Oladnabi M: conceptualization, supervision, writing—review & editing, validation, data curation.

Foundation: Supported by Golestan University of Medical Sciences (No.111294).

Conflicts of Interest: Vahidi A, None; **Khosravi T,** None; **Dastaviz F,** None; **Sheikh Arabi M,** None; **Khosravi A,** None; **Oladnabi M,** None.

REFERENCES

1 Pawar S. Causes of blindness and vision impairment in 2020 and trends over 30 years, and prevalence of avoidable blindness in relation to VISION 2020: the Right to Sight: an analysis for the Global Burden of Disease Study. *SSRN Journal* 2021;9(2):e144-e160.

2 Xu XY, Wu J, Yu XN, Tang YL, Tang XJ, Shentu XC. Regional differences in the global burden of age-related macular degeneration. *BMC Public Health* 2020;20(1):410.

3 Rein DB, Wittenborn JS, Burke-Conte Z, Gulia R, Robalik T, Ehrlich JR, Lundeen EA, Flaxman AD. Prevalence of age-related macular degeneration in the US in 2019. *JAMA Ophthalmol* 2022;140(12): 1202-1208.

4 Fleckenstein M, Keenan TDL, Guymer RH, *et al*. Age-related macular degeneration. *Nat Rev Dis Primers* 2021;7:31.

5 Deng YH, Qiao LF, Du MY, Qu C, Wan L, Li J, Huang LL. Age-related macular degeneration: epidemiology, genetics, pathophysiology, diagnosis, and targeted therapy. *Genes Dis* 2021;9(1):62-79.

6 Formica ML, Awde Alfonso HG, Palma SD. Biological drug therapy for ocular angiogenesis: anti-VEGF agents and novel strategies based on nanotechnology. *Pharmacol Res Perspect* 2021;9(2):e00723.

7 Kaiser SM, Arepalli S, Ehlers JP. Current and future anti-VEGF agents for neovascular age-related macular degeneration. *J Exp Pharmacol* 2021;13:905-912.

8 Campa C, Harding SP. Anti-VEGF compounds in the treatment of neovascular age related macular degeneration. *Curr Drug Targets* 2011;12(2):173-181.

9 Tenbrock L, Wolf J, Boneva S, Schlecht A, Agostini H, Wieghofer P, Schlunck G, Lange C. Subretinal fibrosis in neovascular age-related macular degeneration: current concepts, therapeutic avenues, and future perspectives. *Cell Tissue Res* 2022;387(3):361-375.

10 Suri R, Neupane YR, Jain GK, Kohli K. Recent theranostic paradigms for the management of age-related macular degeneration. *Eur J Pharm Sci* 2020;153:105489.

11 Kudelka MR, Grossniklaus HE, Mandell KJ. Emergence of dual VEGF and PDGF antagonists in the treatment of exudative age-related macular degeneration. *Expert Rev Ophthalmol* 2013;8(5):475-484.

12 Jaffe GJ, Ciulla TA, Ciardella AP, *et al*. Dual antagonism of PDGF and VEGF in neovascular age-related macular degeneration. *Ophthalmology* 2017;124(2):224-234.

13 Ding K, Eaton L, Bowley D, *et al*. Generation and characterization of ABBV642, a dual variable domain immunoglobulin molecule (DVD-Ig) that potently neutralizes VEGF and PDGF-BB and is designed for the treatment of exudative age-related macular degeneration. *MAbs* 2017;9(2):269-284.

14 Kim BH, Yu HG, Hong IH. Volumetric fluid analysis of fixed monthly anti-VEGF treatment in patients with neovascular age-related macular degeneration. *Int J Ophthalmol* 2023;16(6):909-914.

15 Foss A, Rotsos T, Empeslidis T, Chong V. Development of macular atrophy in patients with wet age-related macular degeneration receiving anti-VEGF treatment. *Ophthalmologica* 2022;245(3):204-217.

16 Tayarani-Najaran Z, Tayarani-Najaran N, Eghbali S. A review of auraptene as an anticancer agent. *Front Pharmacol* 2021;12:698352.

17 Genovese S, Epifano F. Auraptene: a natural biologically active compound with multiple targets. *Curr Drug Targets* 2011;12(3):381-386.

18 Fiorito S, Preziuso F, Sharifi-Rad M, Marchetti L, Epifano F, Genovese S. Auraptene and umbelliprenin: a review on their latest literature acquisitions. *Phytochem Rev* 2022;21(2):317-326.

19 Shiran MR, Mahmoudian E, Ajami A, Hosseini SM, Khojasteh A, Rashidi M, Maroufi NF. Effect of Auraptene on angiogenesis in Xenograft model of breast cancer. *Horm Mol Biol Clin Investig* 2022;43(1):7-14.

20 Toliver T, Chintalapati M, Losso JN. Anti-angiogenic activity of auraptene. *The Journal of Young Investigators* 2011;22(3):67-75.

21 Jang Y, Han J, Kim SJ, *et al*. Suppression of mitochondrial respiration with auraptene inhibits the progression of renal cell carcinoma: involvement of HIF-1α degradation. *Oncotarget* 2015;6(35): 38127-38138.

22 Oladnabi M, Amir Mishan M, Rezaeikanavi M, Zargari M, Najjar Sadeghi R, Bagheri A. Correlation between ELF-PEMF exposure and human rpe cell proliferation, apoptosis and gene expression. *J Ophthalmic Vis Res* 2021;16(2):202-211.

23 Sebaugh JL. Guidelines for accurate EC50/IC50 estimation. *Pharm Stat* 2011;10(2):128-134.

24 Lev PR, Salim JP, Kornblihtt LI, Pirola CJ, Marta RF, Heller PG, Molinas FC. PDGF-A, PDGF-B, TGF beta, and BFGF mRNA levels in patients with essential thrombocythemia treated with anagrelide. *Am J Hematol* 2005;78(2):155-157.

25 Mammoto A, Hendee K, Muyleart M, Mammoto T. Endothelial Twist1-PDGFB signaling mediates hypoxia-induced proliferation and migration of αSMA-positive cells. *Sci Rep* 2020;10:7563.

26 Bruland O, Fluge Ø, Akslen LA, Eiken HG, Lillehaug JR, Varhaug JE, Knappskog PM. Inverse correlation between PDGFC expression and lymphocyte infiltration in human papillary thyroid carcinomas. *BMC Cancer* 2009;9(1):425.

27 Tsarouhas A, Soufla G, Tsarouhas K, Katonis P, Pasku D, Vakis A, Tsatsakis AM, Spandidos DA. Molecular profile of major growth factors in lumbar intervertebral disc herniation: correlation with patient clinical and epidemiological characteristics. *Mol Med Rep* 2017;15(4):2195-2203.

28 Oladnabi M, Bagheri A, Rezaei Kanavi M, Azadmehr A, Kianmehr A. Extremely low frequency-pulsed electromagnetic fields affect proangiogenic-related gene expression in retinal pigment epithelial cells. *Iran J Basic Med Sci* 2019;22(2):128-133.

29 Moghtaderi M, Sedaghatnia K, Bourbour M, *et al*. Niosomes: a novel targeted drug delivery system for cancer. *Med Oncol* 2022;39(12):240.

30 Umbarkar MG. Niosome as a novel pharmaceutical drug delivery: a brief review highlighting formulation, types, composition and application. *Indian J Pharm Educ Res* 2021;55(1s):s11-s28.

31 Ge X, Wei M, He S, Yuan WE. Advances of non-ionic surfactant vesicles (niosomes) and their application in drug delivery. *Pharmaceutics* 2019;11(2):55.

32 Bhandari M, Nguyen S, Yazdani M, Utheim TP, Hagesaether E. The therapeutic benefits of nanoencapsulation in drug delivery to the anterior segment of the eye: a systematic review. *Front Pharmacol* 2022;13:903519.

33 Dorgaleleh S, Naghipoor K, Barahouie A, Dastaviz F, Oladnabi M. Molecular and biochemical mechanisms of human iris color: a comprehensive review. *J Cell Physiol* 2020;235(12):8972-8982.

34 Funk M, Karl D, Georgopoulos M, Benesch T, Sacu S, Polak K, Zlabinger GJ, Schmidt-Erfurth U. Neovascular age-related macular degeneration: intraocular cytokines and growth factors and the influence of therapy with ranibizumab. *Ophthalmology* 2009;116(12):2393-2399.

35 Cabral T, Mello LGM, Lima LH, Polido J, Regatieri CV, Belfort R Jr, Mahajan VB. Retinal and choroidal angiogenesis: a review of new targets. *Int J Retin Vitr* 2017;3:31.

36 Chen XD, Ding GL, Suo Y, Zhu YS, Lu HQ,. Clinical efficacy and changes of serum VEGF-A, VEGF-B, and PLGF after conbercept treating neovascular age-related macular degeneration. *Int J Ophthalmol* 2023;16(9):1489-1495.

37 Kniggendorf V, Dreyfuss JL, Regatieri CV. Age-related macular degeneration: a review of current therapies and new treatments. *Arq Bras Oftalmol* 2020;83(6):552-561.

38 Zheng Q, Hirose Y, Yoshimi N, *et al*. Further investigation of the modifying effect of various chemopreventive agents on apoptosis and cell proliferation in human colon cancer cells. *J Cancer Res Clin Oncol* 2002;128(10):539-546.

39 Bibak B, Shakeri F, Barreto GE, Keshavarzi Z, Sathyapalan T, Sahebkar A. A review of the pharmacological and therapeutic effects of auraptene. *BioFactors* 2019;45(6):867-879.

40 Guinedi AS, Mortada ND, Mansour S, Hathout RM. Preparation and evaluation of reverse-phase evaporation and multilamellar niosomes as ophthalmic carriers of acetazolamide. *Int J Pharm* 2005;306(1-2):71-82.

41 Daneshmand S, Jaafari MR, Movaffagh J, *et al*. Preparation, characterization, and optimization of auraptene-loaded solid lipid nanoparticles as a natural anti-inflammatory agent: *in vivo* and *in vitro* evaluations. *Colloids Surf B Biointerfaces* 2018;164:332-339.

42 Afshari AR, Karimi Roshan M, Soukhtanloo M, *et al*. Cytotoxic effects of auraptene against a human malignant glioblastoma cell line. *Avicenna J Phytomed* 2019;9(4):334-346.

43 Guryanov I, Tennikova T, Urtti A. Peptide inhibitors of vascular endothelial growth factor A: current situation and perspectives. *Pharmaceutics* 2021;13(9):1337.

44 Momekova DB, Gugleva VE, Petrov PD. Nanoarchitectonics of multifunctional niosomes for advanced drug delivery. *ACS Omega* 2021;6(49):33265-33273.

45 Rinaldi F, Del Favero E, Rondelli V, *et al*. pH-sensitive niosomes: effects on cytotoxicity and on inflammation and pain in murine models. *J Enzyme Inhib Med Chem* 2017;32(1):538-546.